

## Article

# Ecoflex Flexible Array of Triboelectric Nanogenerators for Gait Monitoring Alarm Warning Applications

Qinglan Zheng<sup>1</sup>, Changjun Jia<sup>1</sup>, Fengxin Sun<sup>1</sup>, Mengqi Zhang<sup>1</sup>, Yuzhang Wen<sup>1</sup>, Zhenning Xie<sup>1</sup>, Junxiao Wang<sup>2</sup>, Bing Liu<sup>3,\*</sup>, Yupeng Mao<sup>1,2,\*</sup>  and Chongle Zhao<sup>1,\*</sup> 

- <sup>1</sup> Physical Education Department, Northeastern University, Shenyang 110819, China; 2271515@stu.neu.edu.cn (Q.Z.); 2071367@stu.neu.edu.cn (C.J.); 2171435@stu.neu.edu.cn (F.S.); 2201367@stu.neu.edu.cn (M.Z.); 2201361@stu.neu.edu.cn (Y.W.); 2201362@stu.neu.edu.cn (Z.X.)
- <sup>2</sup> School of Strength and Conditioning Training, Beijing Sport University, Beijing 100084, China; m15753191782@163.com
- <sup>3</sup> School of Martial Arts and Dance, Shenyang Sport University, Shenyang 110102, China
- \* Correspondence: bingliu067@163.com (B.L.); maoyupeng@pe.neu.edu.cn (Y.M.); zhaochongle@pe.neu.edu.cn (C.Z.)

**Abstract:** The advent of self-powered arrays of tribological nanogenerators (TENGs) that harvest mechanical energy for data collection has ushered in a promising avenue for human motion monitoring. This emerging trend is poised to shape the future landscape of biomechanical study. However, when we try to monitor various regions of the foot across disparate environments simultaneously, it poses a number of problems, such as the lack of satisfactory waterproofing, suboptimal heat resistance, inaccurate monitoring capacity, and the inability to transmit data wirelessly. To overcome these issues, we have developed an array of sensors affixed to the insole's surface to adeptly monitor movement gait patterns and alert users to falls using self-powered triboelectric nanogenerators (TENGs). Each sensor cell on this sensor works as an individual air gap TENG (FWF-TENG), namely flexible, waterproof, and fast response, composed of an Ecoflex single-electrode array. Each FWF-TENG boasts a fast response time of 28 ms, which is sufficient to quickly monitor pressure changes during various badminton activities. Importantly, these sensors can persistently generate electrical signals at 70%RH humidity. Data obtained from these sensors can be transmitted to an upper computer intelligent terminal wirelessly through multi-grouped FHW-ENG sensing terminals in real time to achieve human–computer interaction applications, including motion technical determinations, feedback, and fall alerts. As a result, the interconnected TENG arrays have broad potential applications, including gait rehabilitation monitoring, motion technique identification, and fall alarm applications.

**Keywords:** triboelectric nanogenerator; human mechanical energy collection; movement monitoring; rehabilitation monitoring



**Citation:** Zheng, Q.; Jia, C.; Sun, F.; Zhang, M.; Wen, Y.; Xie, Z.; Wang, J.; Liu, B.; Mao, Y.; Zhao, C. Ecoflex Flexible Array of Triboelectric Nanogenerators for Gait Monitoring Alarm Warning Applications. *Electronics* **2023**, *12*, 3226. <https://doi.org/10.3390/electronics12153226>

Academic Editor: Enzo Pasquale Scilingo

Received: 27 June 2023  
Revised: 19 July 2023  
Accepted: 20 July 2023  
Published: 26 July 2023



**Copyright:** © 2023 by the authors. Licensee MDPI, Basel, Switzerland. This article is an open access article distributed under the terms and conditions of the Creative Commons Attribution (CC BY) license (<https://creativecommons.org/licenses/by/4.0/>).

## 1. Introduction

With the advent of the 5G era, we have seen rapid economic growth along with a steady improvement in quality of life. These developments have brought the concept of comprehensive health to the forefront of discussion [1–4]. Currently, exercise is regarded as one of the most effective ways to enhance one's health status [5–8]. However, clinical analysis of racket-sport injuries shows a high incidence in the lower extremities, making up over 58% of cases, with a particular emphasis on the knees and ankles [9–13]. Nowadays, badminton is gaining popularity, and significantly emphasizes footwork as a critical part of its technique [14–18]. Monitoring the exact pace of a game not only allows for fast and efficient returns but also lowers the risk of injuries [19,20]. As such, badminton gait analysis can be used as a valuable tool for diagnosing motor skills and enhancing training program optimization [21–23]. Additionally, gait analysis has been employed in fields like medical rehabilitation and other fields [17,24–27]. It is particularly useful

for studying pathological gait, the gait of the elderly, and other related areas [28,29]. In order to integrate multiple applications into a single device, gait analysis employs a variety of strategies and mechanisms related to optical imaging systems [30]. However, the application of conventional instruments, despite providing impressive accuracy, is marred by drawbacks such as high costs, operational complexity, and the necessity of an external power supply. Consequently, the development of wearable [31–34], flexible [35–38], cost-effective [39–42], and recognition-precise [43–46] gait analysis tools continues to pose significant challenges [47–50].

Recently, triboelectric nanogenerators (TENGs) have found applications in mechanical energy harvesting and self-powered sensors to track an array of motion [31]. They utilize contact charging and electrostatic induction for coupling effects, converting mechanical energy into electrical energy [51–53]. Owing to their multiple advantages such as being maintenance-free, biocompatible, and offering a broad range of material options, TENGs have become a popular choice. In terms of blue energy, a frictional electric nanogenerator based on 3D-printing technology combined with PTFE has been reported as an option for human motion energy harvesting and associated gait monitoring [7]. However, this sensor lacks gait differentiation capabilities and only monitors associated motion based on frequency. Additionally, a friction nanogenerator, based on a combination of EAC and rubber, has been investigated for application in medical rehabilitation to monitor gait abnormalities and serve as an fall alarm system [54]. However, because this sensor does not boast a high output, nor does it integrate machine learning capabilities, there still remains a dearth of studies on the accuracy and visual learning of TENGs in gait analysis.

To address the aforementioned issues, this study embarked on the development of a flexible, recognition-accurate, and self-powered smart insole based on tribological nanogenerators with flexibility, waterproofing, and swift response characteristics (FWF-TENG) and which is designed for real-time, multifunctional gait analysis [55]. The smart insole consists an array of four friction sensors. Each individual friction sensor is constructed of a silicon Ecoflex and a copper layer. The copper layer, embedded within the external rubber layer, reduces invalid signals caused by environmental factors, and the rubber layer is waterproofed to prevent sweat-induced contamination of the device's transmission signal. Each friction electrode sensor generates an air gap through the vaporization of deionized water, thus eliminating the need for a liner [56,57]. The sensor demonstrates a swift response of 28 ms and can still generate an electrical signal at 70% RH humidity. This paper employs an array to connect the four independent sensors. The smart insole, composed of this sensor array, facilitates more accurate gait measurements, and, in addition, by monitoring the change in the single-support phase during gait analysis, it can accurately track the progression of disease treatment or the status of the user's health. Through the contact between each section of the foot and the array insole, the use of gait information combined with the upper computer can realize multi-point deployment; this enables the identification and analysis of various gait patterns and accurately determines the application of force to the specific part of the foot. Of paramount importance is the smart insole's ability to monitor and instantly alert users to accidental fall events. With its characteristics of wearability, being self-powering, flexibility, cost-effectiveness, and accurate recognition, the smart array insole provides a more convenient solution for human gait analysis and evaluation. It has wide-ranging potential for applications in motion recognition and healthcare systems.

## 2. Materials and Methods

### 2.1. Materials

The smooth Ecoflex 00-30 was purchased from Beijing Lancheng Fanfei Technology Co., Ltd. (Beijing, China). Conductive copper foil was purchased from Dongguan Chengyu Adhesive Products Co., Ltd. (Dongguan, China). Microporous copper foil (single-sided gross) purchased from Shanghai Gaxian Metal Materials Co., Ltd. (Shanghai, China). FEP perfluoroethylene propylene copolymer purchased from Jiangsu Fountain Material

Technology Co., Ltd. (Zhenjiang, China). Enamelled wire purchased from Shenzhen Hao Li You Times Electronic Tools Co., Ltd. (Shenzhen, China).

## 2.2. Preparation of Ecoflex Mixed Glues Solution

(1) Mix Ecoflex A gum solution with Ecoflex B gum solution in a 1:1 ratio for a total of 20 g. (2) Stir for 15 min to ensure that the Ecoflex gum solution is completely mixed. (3) Ultrasonically shake the mixed gum was for 5 min and leave to stand for 10 min to obtain a bubble-free mixture.

## 2.3. Fabrication of the FWF-TENG

(1) Casting preparation: Use a knife to cut the perfluoroethylene propylene copolymer (FEP) to a size of 5 cm × 4 cm × 0.01 cm. (2) Pour the Ecoflex glue-mixture solution into the base plate, and then move the base plate to an oven at 80 °C. When the glue solution is fully cured, a 3 cm × 3.5 cm Ecoflex mixture substrate is formed. (3) Pour the Ecoflex mixture solution into the substrate, and then move the substrate to an oven at 80 °C until it becomes semi-solidified. (4) Cut the two copper foils to a size of 3 cm × 3 cm and place on the mixture substrate with the non-glossy side facing up. Then, flatten the copper foil surface with 2 μL of deionized water. Note that the copper foil is hydrophilic because it is roughened. The water droplets on the copper foil are evenly distributed and the overall thickness of the FWF-TENG is reduced. Connect the enamelled wire between the two copper foils as a connecting wire. (5) Pour the Ecoflex mix onto the base plate again so that the glue completely seals the deionized water and the copper foil. Transfer the device to an oven and heat at 80 °C for 10 min. (6) Finally, pour the Ecoflex glue mix again into the base plate for the final full sealing of the device, transfer to an oven and heat at 105 °C for 12 h to completely turn the deionized water in the device into water vapor. For the specific production process of FWF-TENG, please refer to Figure 1b.

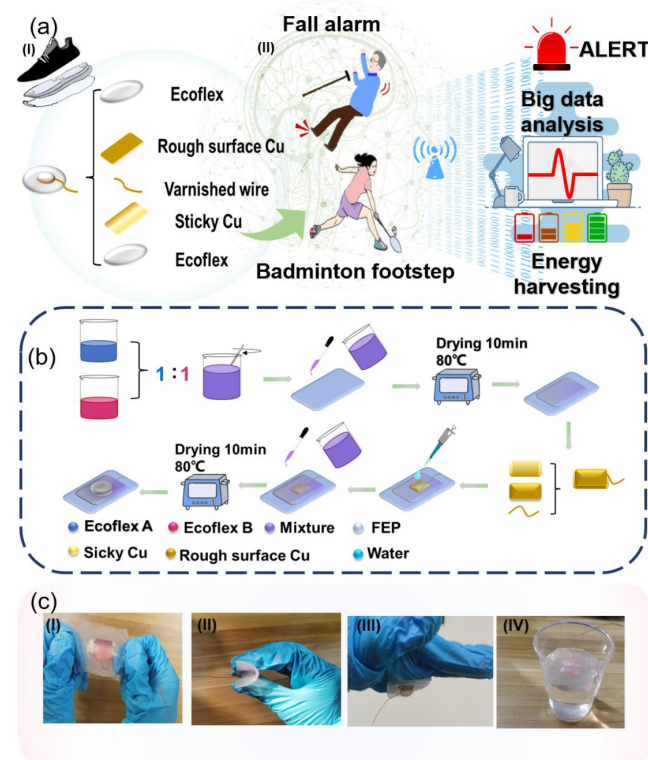


**Figure 1.** Design of gait analysis in badminton. (a) Schematic diagram of FWF-TENG applied as a smart insole for human gait analysis monitoring. (I) shows the structure of FWF-TENG. (II) Demonstrates the functions of the FWF-TENG. (b) Production process of FWF-TENG. (c) Optical image of FWF-TENG (I) stretchability, (II) foldability, (III) adhesiveness, and (IV) light weight.

#### 2.4. Characterization and Measurements

Fix the FWF-TENG to the acrylic fixing frame opposite the stepping motor with adhesive tape. Figure S1a shows the working diagram of FWF-TENG simulated by a stepper motor. Simulate the motion using the frequency and amplitude set by the stepper motor control system. Collect the signals generated by the sensors with an oscilloscope (sto1102c, Shenzhen, China). Oscilloscope display diagram in Figure S1b. The oscilloscope was connected to the stepping motor.

### 3. Results

Figure 1a shows a schematic of the FWF-TENG being used for gait monitoring. (I) shows the structure of the FWF-TENG. The FWF-TENG consisted of Ecoflex, rough surface copper, varnished copper, and tacky copper. The inside was evaporated by water vapor as an air supporting layer. The composition of four independent sensors in the form of an array allowed for more accurate monitoring of gait information. (II) Demonstrates the functions of the FWF-TENG. The FWF-TENG can be used as a portable sensor in the form of an array of insoles to collect the energy generated by human gait and convert it into mechanical energy. In addition, the FWF-TENG can monitor human movement information, badminton gait determination, and real-time fall alarm through big data analysis. Figure S2 provides an optical picture of the FWF-TENG array located in the insole. The production technology of the FWF-TENG is shown in Figure 1b. First, we made the Ecoflex glue solution, and then sealed the copper electrode on PET with the mixed solution. The deionized water evaporated to form a gas support layer. The production process is detailed in Section 2. Figure 1c is an optical photograph of the FWF-TENG in its stretchability (I), foldability (II), adhesiveness (III), and light-weight (IV) states, demonstrating that the device fits well to the human foot surface. The supporting gas layer can be clearly observed in Movie S1.

Figure 2a shows the working mechanism of the smart insole. A single electrode mode operating mechanism was used. Cu obtained a positive surface charge and rubber obtained a negative surface charge based on their position on the triboelectric series of materials. When the rubber layer approached the copper layer, the potential of the copper electrode decreased and electrons flowed from the copper layer to the ground. When the rubber was in complete contact with the copper, an equal and opposite charge was generated. Conversely, when the rubber layer left the copper layer, the potential of the copper electrode rose and electrons flowed from the ground back to the copper electrode. In order to understand the working mechanism of the sensor in detail, Figure 2b shows a simulation of the potential distribution from the COMSOL software.

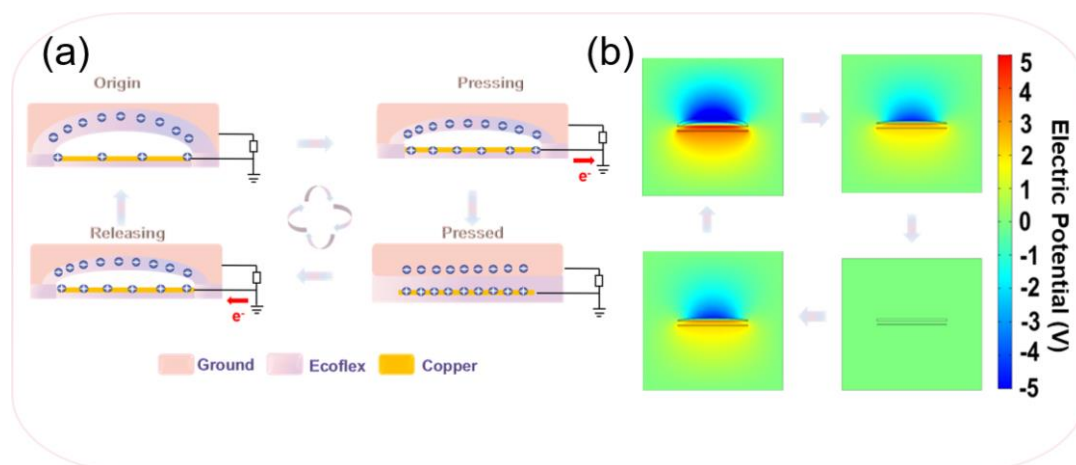


**Figure 2.** Mechanism principle of FWF-TENG. (a) Mechanism of FWF-TENG operation. (b) COMSOL simulation of FWF-TENG friction potential.

The analysis of gait can help the body to accomplish movement and rehabilitation. Different foot landings and power generation determine the form of movement as well as the position of recovery. In badminton, due to irregular gait technical motion and blind pursuit of effects, it can cause excessive pressure on the knees and ankles, which can easily bring the risk of injury. Additionally, beginners' technical motions are too rough, and blind force can easily cause joint injuries. To overcome these issues, we developed a flexible, recognition-accurate, as well as self-powered smart insole (FWF-TENG) based on a nano-friction generator for real-time multifunctional gait analysis. Therefore, to ensure that the FHW-TENG can meet real-world motion requirements, we utilized stepper motors to simulate joint motion processes. The performance of a single closed TENG relies on various structural factors that have been investigated to optimize its output performance. The platform that was used to test the properties of the TENG is illustrated in Figure 3a. Figure 3b shows the simulated human motion frequency and, thus, the calculation of the instantaneous force of the TENG. The drop time  $t_1$  is calculated according to Equation (1), counting the force in contact with the device (2) with a default contact time " $t_2$ " of 0.1 s:

$$t_1 = \sqrt{\frac{2h}{g}} \quad (1)$$

$$F = \frac{mgt_1}{t_2} \quad (2)$$

where  $m$  denotes the substance;  $g$  is the default acceleration of gravity, 10; and  $h$  is the height of the fall, and is achieved by a stepper motor-controlled motion frequency, a simple pulley set, and multiple counterweight blocks at a frequency of 1 Hz. It has been shown that higher forces lead to better contact between the elastic rubber layer and the copper layer, and, therefore, to higher electrical output. For example, when using the lowest applied force (2 N), the voltage output was 4.9 V; however, when using the highest applied force (8 N), the voltage output rose to 19.9 V. These results also mean that it can detect very low external forces (2 N). In addition to the force aspect, it is also crucial to determine the dimensions, as shown in Figure 3c. Comparing a 3 cm × 3.5 cm TENG with a 1 cm × 1.5 cm TENG at the same humidity and frequency, it clearly shows that the voltage of the 3 cm × 3.5 cm is higher than that of the 1 cm × 1.5 cm. The 3 cm × 3.5 cm TENG is not only more comfortable and accommodates for human feet of different sizes, but also has a larger contact area and voltage generated. As can be seen in Figure 3c, the output voltage of the FWF-TENG is shown for the same force, same humidity, and different frequency conditions. As can be seen in Figure 3d, the average output voltage was 3.1 V, 2.9 V, 2.7 V, and 3.1 V when the frequencies were 0.5 Hz, 1 Hz, 1.5 Hz, and 2 Hz, respectively, indicating that the FWF-TENG has good stability during the monitoring of low-frequency motion. The monitoring of motion frequency is of great importance for motion-sensing monitoring. Kinematic ability affects the frequency of body motions and their completion quality. The response of the FWF-TENG at different frequencies is shown in Figure 3e. The response can be calculated using the following, Equation (3):

$$R\% = \left| \frac{(V_0 - V_i)}{V_i} \right| \times 100\% \quad (3)$$

where  $V_i$  is the output voltage at 0.5 Hz and  $V_0$  is the output voltage at other frequencies. When the FWF-TENG operated at 0.5 Hz, 1 Hz, 1.5 Hz, and 2 Hz under the same strength, same temperature, and different frequency conditions, the responses of the corresponding outputs were 0%, 1%, 1.5%, and 0%, respectively. The output voltage of the FWF-TENG hardly varied with the motion frequency, indicating that in actual badminton, it can accurately monitor the change in motion frequency. Figure 3f shows the fast response of the FWF-TENG at about 28 ms. Table S1 demonstrates that the FWF-TENG response was faster compared to other TENG responses. Other sensors can transmit data to the host

computer in real time for coaches to analyze and grasp the athletes' sports status in time for effective motion-technique diagnosis. Meanwhile, the signal control system provides a guarantee for realizing human–computer interaction gait accuracy judgment. Figure 3g shows the output voltage of the FWF-TENG under different humidity levels. The average output voltages were 1.76 V, 1.76 V, 2.36 V, and 1.43 V when the humidity was 40% RH, 50% RH, 60% RH, and 70% RH, respectively, indicating that the FWF-TENG has good water resistance. It shows that the sweat produced by the direct contact between the FWF-TENG and skin does not affect the voltage output of the FWF-TENG. To show that the Ecoflex material has good water resistance, Figure 3h compares the TENG containing Ecoflex with the TENG without Ecoflex at 70% RH humidity, and the voltage with Ecoflex is more than 400 times higher than without Ecoflex. Figure 3i shows the stability test of the sensor under continuous operation for 2400 s, and its output voltage can be stabilized at 3.5 V for daily training applications. These results above show that the FWF-TENG has good electrical performance and has great potential in self-powered sensing and self-powered systems.

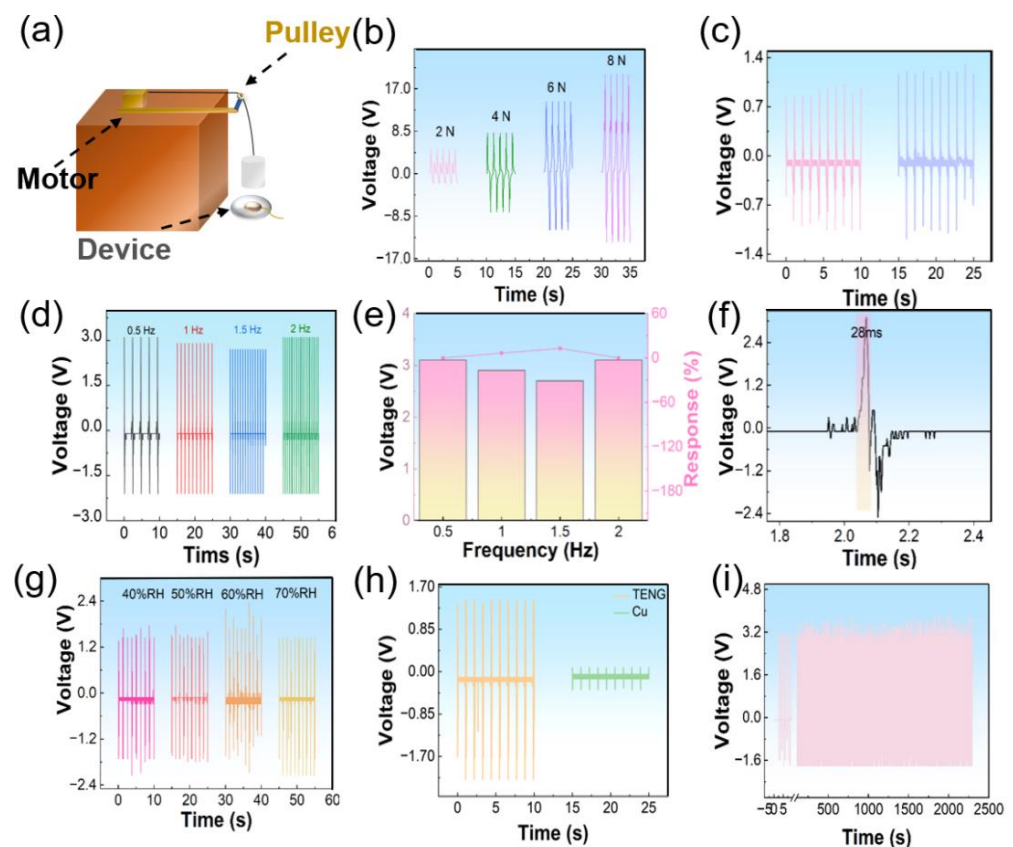


**Figure 3.** Performance testing and selection of the FWF-TENG. (a) Test bench of the FWF-TENG. (b) Voltage at different forces of the FWF-TENG. (c) 3 cm × 3.5 cm TENG (purple) and 1 cm × 1.5 cm TENG (pink) Comparison of output voltages for different sizes. (d) Output voltage of the FWF-TENG at different frequencies. (e) Voltage response of the FWF-TENG at different frequencies. (f) Real-time fast response time of the FWF-TENG. (g) Output voltage of the FWF-TENG at different humidity conditions. (h) Output voltage of the FWF-TENG with different materials at the same humidity. (i) Durability test of the FWF-TENG for 2400 s conditions.

The good low-frequency mechanical energy harvesting capability of the FWF-TENG is guaranteed for WPIS (Wireless Precision Intelligence System) applications (Figure 4). Figure S3 demonstrates the full form of the WPIS. The WPIS is mainly converted from mechanical energy to electrical energy by sensors (FWF-TENG). The electrical signal is transmitted to the AD module, which is mainly composed of Bluetooth, Amplifier, Low-Pass Filters. The signal from the transmitting end of the AD module is then transmitted

to the Bluetooth on the receiving end and uploaded to the upper computer. We used the fast Fourier Transform-located port for the judgment of gait-related information. Accurate amplitude transformation was performed on the input signal to complete the recognition of motion information. The system can clearly recognize the accuracy of the front pad step force and the upper computer in the form of animated real-time feedback success and failure. The upper computer contains a motion-information judgment system to control the threshold size for intelligent judgment. Figure 4a shows the equivalent circuit diagram of the FWF-TENG. The switch controls the switching of the charging and discharging modes. The capacitor acts as an energy storage. When the current is introduced into the rectifier, the AC current can be converted into DC current. Figure 4b illustrates the variation of the output voltage and the calculated current signal of the FWF-TENG measured at 1 to 35 MΩ load resistors. We can calculate  $I$  by using the following, Formula (4):

$$I = \frac{V}{R} \quad (4)$$

where  $I$  stands for current,  $V$  stands for voltage, and  $R$  stands for resistance. It is clearly demonstrated that as the load resistor increases, the voltage increases, while the current decreases. Figure 4c shows the output power of the FWF-TENG at different load resistances. We can calculate the power by using the following, Formula (5):

$$P = \frac{V^2}{R} \quad (5)$$

where  $P$  stands for power in the formula, while  $V$  stands for voltage and  $R$  stands for resistance. The FWF-TENG provides the maximum power output at a resistance of 20 MΩ. The charging voltage increases as the frequency of motion increases. Figure 4f illustrates the voltage-time curves of the FWF-TENG charging different capacitors. Briefly, 1 μF, 2.2 μF, and 4.7 μF capacitors can be charged to 7.9 V, 2.5 V, and 1.4 V, respectively, after 11 s. The FWF-TENG can provide stable and sustainable energy for wearable or portable electronic devices without an external energy supply. As shown in Figure 4e and Movie S2, showing the FWF-TENG charge/discharge curve for powering an electronic watch, the FWF-TENG can charge a 4.7 μF capacitor to power an electronic watch using a stepper motor at a constant and stable frequency. Additionally, the capacitor can be charged to 2.2 V in about 4.6 s to repeatedly power the watch. In addition, Figure 4f shows the real-time application capability of the FWF-TENG. The “Z” series of green LEDs can be lit by tapping the FWF-TENG with your hand. Inspired by the good low-frequency mechanical energy harvesting capability of the FWF-TENG, it has good promise as a biomechanical energy harvester to power electronics.

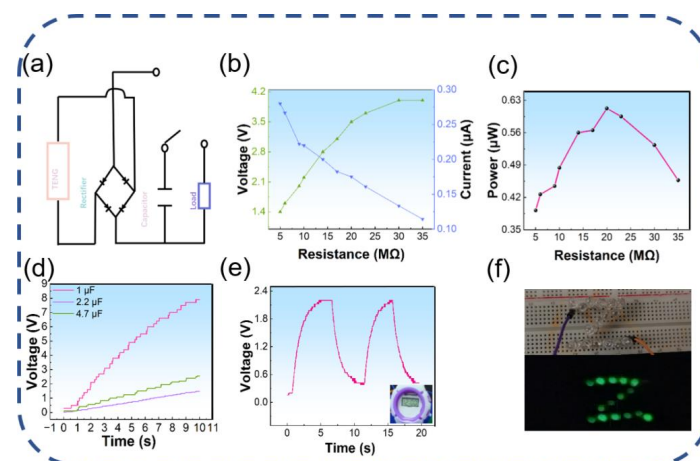


**Figure 4.** Frictional electrical performance of FWF-TENG. (a) Equivalent circuit diagram of FWF-TENG charging and discharging. (b) Correlation of output voltage and current at different load

resistances. (c) Power dependence at different load resistances. (d) Charging performance of capacitors at different loads. (e) Charging and discharging the electronic watch with capacitors. (f) Lighting the “Z” commercial LED with a light tap.

Figure 5a shows that a wireless transmission system for self-powered sensors has been created to make it easier to apply the FWF-TENG in practice. An optical picture of the FHW-TENG’s wireless transmission system is shown in Figure S4. Badminton movement monitoring was the movement action net lift of the front pad step generated by the electrical signal and transmitted to the WPIS for intelligent judgment. Among other things, the Bluetooth device requires an external power supply to power it. The problem of gait rehabilitation is still valued by society, where different foot force points lead to different responses from the body. Figure 5b and Movie S3 show the real-time monitoring of different foot force points and the generated signal response. The toe-first landing state and the electrical signals generated by the four arrays of TENG units can be seen in Figure 5b(I). Toe-first landing tends to cause cross-domain gait. The main cause of toe dragging with foot drop and increased hip flexion and knee flexion during the swing phase is weakness of the ankle dorsiflexors. Additionally, Figure 5b(II,III) can also clearly demonstrate its related signals through the chart. The force from both sides tends to cause the weight to shift to the ipsilateral side, so that the unilateral lower limb supports the body weight, and patients with hemiplegia, joint pain, and low balance tend to have too short a time. Figure 5b(IV), in which the foot follows the ground, can also demonstrate the relevant signal from the chart. Heel landing tends to lead to increased tension in the extensor muscles of the lower extremity, making it difficult for patients with foot drop and pronation to complete the movement. First, the FWF-TENG was connected to a commercial LED array and used four LEDs to display the corresponding position of the gait in order to visualize the monitoring signal. Stress mapping data were collected for each gait condition by human motion. It can be seen that the distribution of the data signal was consistent with the specified gait condition. In addition, the FWF-TENG output electrical signals can be clearly distinguished and monitored in real time at different gait phases. It can be observed that the optical mapping profile of the LED array was consistent with both the stress and electrical mapping results, and the LED array can directly reflect local variations in gait phase changes, demonstrating the feasibility of using the FWF-TENG as a self-powered and wearable gait-phase visualization platform. Since badminton requires non-stop sport on a relatively narrow field, a large percentage of athletes currently suffer losses to lower-limb joints due to the footwork of badminton not being properly mastered. The WPIS prepares a motion-information judgment function to monitor the standard of the front pad movement in order to make the player’s picking action more adequate. The FWF-TENG sensing end transmits gait-related information wirelessly to the upper computer intelligent judgment end, and the port is used to determine the gait-related information by using fast Fourier transform. The signal input is precisely transformed in terms of amplitude to complete the recognition of motion information. The system is able to clearly identify the accuracy of the force applied during the front cushion step, and is given real-time feedback in the form of real-time animations of success and failure by the upper computer (Video S4). Figure 5c shows an image of the incorrect force and the corresponding data, in which it is clear that the voltage generated by the forefoot landing is higher than the voltage generated by the other three gait positions. Figure 5d shows an image of the correct front pad step and the corresponding data, in which it is clear that the voltage produced by the heel is higher than the voltage produced by the remaining three gait positions. Therefore, the smart insole can also use the mechanical energy generated by the gait and the related data obtained to transmit to the upper computer intelligent port, which uses the data at the time of signal input to identify the amplitude value generated and the occurrence of threshold abnormalities to achieve real-time alarms. It can be used to monitor fall events. First, Figure 5e monitors the typical walking gait signal measured. As shown in Figure 5f and Video Movie S5, the fall situation is monitored and a real-time alarm is achieved.

This study demonstrates the great potential of our smart insoles for motion monitoring as well as medical applications, especially for real-time monitoring of motion gait and emergency medical alert systems for patients. With the continuous advancement of gait-related monitoring, future monitoring systems can visualize the data generated by the human body through movement into 3D images, providing a great aid to the improvement of sports technology.

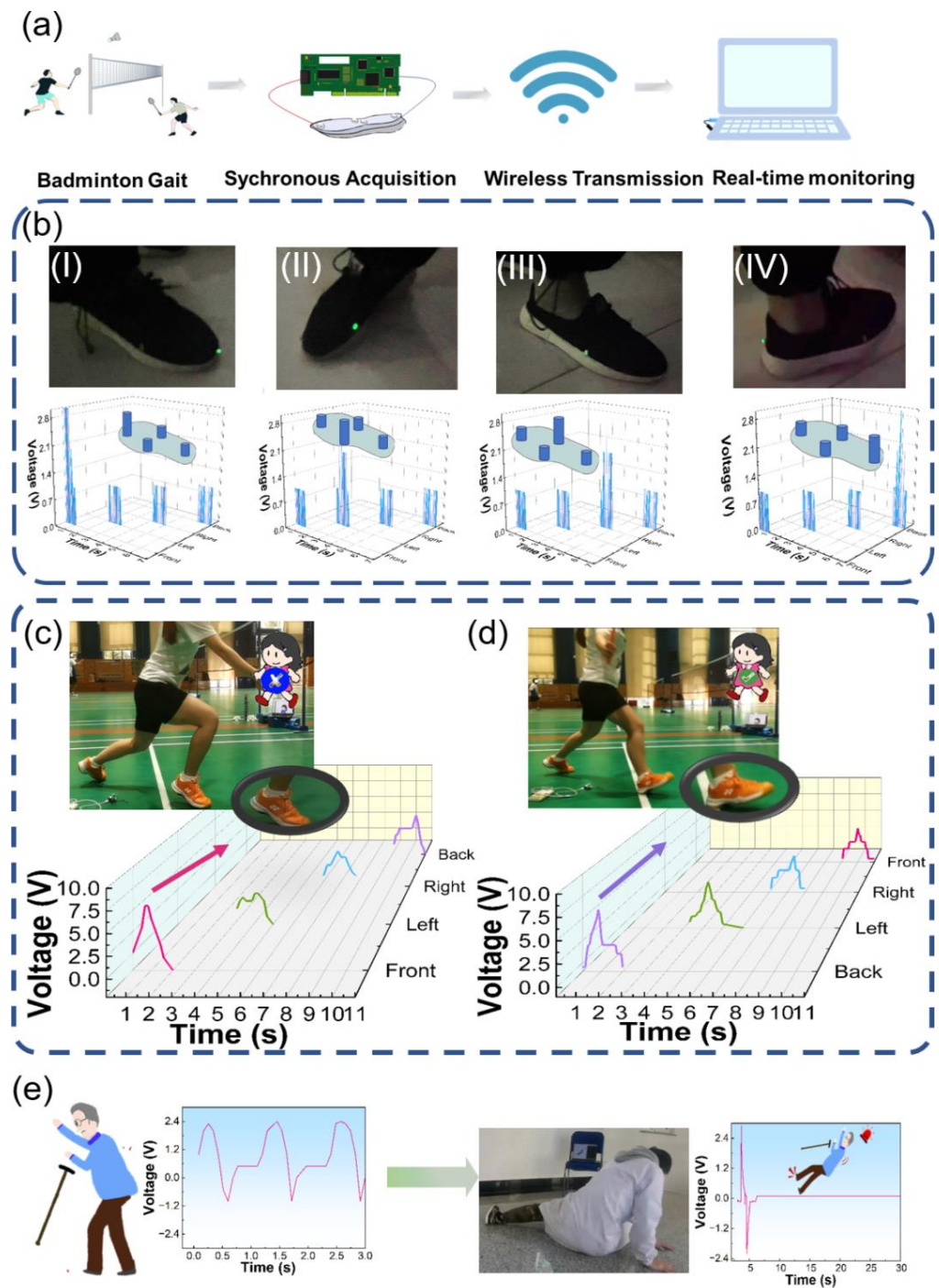


**Figure 5.** WPIS smart insole monitoring application. (a) WPIS technical analysis scheme diagram. (b) Self-powered gait phase visualization platform. (I) forefoot landing. (II) and (III) right and left side landing. (IV) heel landing. (c) Intelligent judgment of toe landing in badminton front pad stance. (d) Badminton front pad stepping with heel intelligent judgment of landing. (e) Fall alarm.

#### 4. Conclusions

In conclusion, we designed a WPIS, a self-powered system capable of transforming mechanical energy into electrical energy for motion monitoring. This system, paired with intelligent analysis capabilities at the end of the upper computer, serves as a determinant for the technique of front pad motion in badminton, as well as providing a fall alarm system. Through flexible FHW-TENG array sensing, our system accomplishes the following: (1) It features a unique, waterproof structure, ensuring that impurity pollution does not impact the performance of the FWF-TENG. (2) The FWF-TENG sensing end is self-powered, eliminating the need for an external power supply; this allows for the flexible and portable collection of mechanical energy generated by human movement. (3) It offers real-time collection of movement information, swiftly providing feedback to the computer side. This is ideal for simple human–computer interaction applications, as well as for determining badminton sport techniques and fall alarms. This multidisciplinary research represents a significant advance in sports science and gait monitoring. Nevertheless, other challenges persist. Future monitoring systems could transform data generated by human movement into visual 3D images, providing a substantial aid to the improvement of sports technology.

**Supplementary Materials:** The following supporting information can be downloaded at: <https://www.mdpi.com/article/10.3390/electronics12153226/s1>, Table S1: Comparison between FWF-TENG response and fast response of other TENGs; Figure S1: Measurement equipment; Figure S2: Optical picture of the FWF-TENG array form located in the insole; Figure S3: Demonstrates the full form of the WPIS; Figure S4: Optical picture of the FWF-TENG's wireless transmission system; Video S1: Demonstration of the gas support structure of the FWF-TENG; Video S2: FWF-TENG lights LEDs; Video S3: LEDs on each part of the foot are accurately lit by the sensor; Video S4: Badminton gait wireless judgment; Video S5: Real-time fall alarm.

**Author Contributions:** Conceptualization, Y.M. and C.Z.; methodology, C.J.; software, M.Z.; validation, Y.W., Q.Z. and Z.X.; formal analysis, M.Z.; investigation, C.J.; resources, Y.W.; data curation, Z.X.; writing—original draft preparation, Q.Z.; writing—review and editing, Q.Z.; visualization, F.S.; supervision, B.L.; project administration, F.S.; funding acquisition, J.W. All authors have read and agreed to the published version of the manuscript.

**Funding:** This research was supported by “the Fundamental Research Funds for the Central Universities” (N2321001) and the “Research on the development and application of college sports” of the China Higher Education Association (21TYB16).

**Data Availability Statement:** The data presented in this study are available in the Supplementary Materials.

**Acknowledgments:** The authors would like to thank the collaboration of all volunteers who participated in data collection.

**Conflicts of Interest:** The authors declare no conflict of interest.

#### References

1. Yang, D.; Ni, Y.; Kong, X.; Li, S.; Chen, X.; Zhang, L.; Wang, Z.L. Self-Healing and Elastic Triboelectric Nanogenerators for Muscle Motion Monitoring and Photothermal Treatment. *ACS Nano* **2021**, *15*, 14653–14661. [[CrossRef](#)] [[PubMed](#)]
2. Li, X.; Tao, J.; Guo, W.; Zhang, X.; Luo, J.; Chen, M.; Zhu, J.; Pan, C. A self-powered system based on triboelectric nanogenerators and supercapacitors for metal corrosion prevention. *J. Mater. Chem. A* **2015**, *3*, 22663–22668. [[CrossRef](#)]
3. Hasan, M.; Bin Sadeque, S.; Albasar, I.; Pecenek, H.; Dokan, F.K.; Onses, M.S.; Ordu, M. Scalable Fabrication of MXene-PVDF Nanocomposite Triboelectric Fibers via Thermal Drawing. *Small* **2023**, *19*, 2206107. [[CrossRef](#)] [[PubMed](#)]
4. Tat, T.; Libanori, A.; Au, C.; Yau, A.; Chen, J. Advances in triboelectric nanogenerators for biomedical sensing. *Biosens. Bioelectron.* **2021**, *171*, 112714. [[CrossRef](#)]
5. Sun, F.; Zhu, Y.; Jia, C.; Ouyang, B.; Zhao, T.; Li, C.; Ba, N.; Li, X.; Chen, S.; Che, T.; et al. A Flexible Lightweight Triboelectric Nanogenerator for Protector and Scoring System in Taekwondo Competition Monitoring. *Electronics* **2022**, *11*, 1306. [[CrossRef](#)]
6. Zhu, Y.; Sun, F.; Jia, C.; Zhao, T.; Mao, Y. A Stretchable and Self-Healing Hybrid Nano-Generator for Human Motion Monitoring. *Nanomaterials* **2021**, *12*, 104. [[CrossRef](#)]
7. Mao, Y.; Zhu, Y.; Zhao, T.; Jia, C.; Wang, X.; Wang, Q. Portable Mobile Gait Monitor System Based on Triboelectric Nanogenerator for Monitoring Gait and Powering Electronics. *Energies* **2021**, *14*, 4996. [[CrossRef](#)]

8. He, M.; Du, W.; Feng, Y.; Li, S.; Wang, W.; Zhang, X.; Yu, A.; Wan, L.; Zhai, J. Flexible and stretchable triboelectric nanogenerator fabric for biomechanical energy harvesting and self-powered dual-mode human motion monitoring. *Nano Energy* **2021**, *86*, 106058. [[CrossRef](#)]
9. Chard, M.D.; Lachmann, S.M. Racquet sports--patterns of injury presenting to a sports injury clinic. *Br. J. Sports Med.* **1987**, *21*, 150–153. [[CrossRef](#)]
10. Bahr, R.; Krosshaug, T. Understanding injury mechanisms: A key component of preventing injuries in sport. *Br. J. Sports Med.* **2005**, *39*, 324–329. [[CrossRef](#)]
11. Boesen, A.P.; Boesen, M.I.; Koenig, M.J.; Bliddal, H.; Torp-Pedersen, S.; Langberg, H. Evidence of accumulated stress in Achilles and anterior knee tendons in elite badminton players. *Knee Surg. Sports Traumatol. Arthrosc.* **2011**, *19*, 30–37. [[CrossRef](#)]
12. Marchena-Rodriguez, A.; Gijon-Nogueron, G.; Cabello-Manrique, D.; Ortega-Avila, A.B. Incidence of injuries among amateur badminton players: A cross-sectional study. *Medicine* **2020**, *99*, e19785. [[CrossRef](#)] [[PubMed](#)]
13. ChangSheng, Z.; Shin, H.-K.; Kim, Y.S. Study on the Injury and Rehabilitation of Racket Athletes with Disabilities. *J. Korean Phys. Ther.* **2019**, *31*, 228–235. [[CrossRef](#)]
14. Muro-De-La-Herran, A.; Garcia-Zapirain, B.; Mendez-Zorrilla, A. Gait Analysis Methods: An Overview of Wearable and Non-Wearable Systems, Highlighting Clinical Applications. *Sensors* **2014**, *14*, 3362–3394. [[CrossRef](#)] [[PubMed](#)]
15. Yang, P.; Shi, Y.; Li, S.; Tao, X.; Liu, Z.; Wang, X.; Wang, Z.L.; Chen, X. Monitoring the Degree of Comfort of Shoes In-Motion Using Triboelectric Pressure Sensors with an Ultrawide Detection Range. *ACS Nano* **2022**, *16*, 4654–4665. [[CrossRef](#)]
16. Xu, X.; Chen, Y.; He, P.; Wang, S.; Ling, K.; Liu, L.; Lei, P.; Huang, X.; Zhao, H.; Cao, J.; et al. Wearable CNT/Ti3C2Tx MXene/PDMS composite strain sensor with enhanced stability for real-time human healthcare monitoring. *Nano Res.* **2021**, *14*, 2875–2883. [[CrossRef](#)]
17. Pollock, A.; Baer, G.; Campbell, P.; Choo, P.L.; Forster, A.; Morris, J.; Pomeroy, V.M.; Langhorne, P. Physical rehabilitation approaches for the recovery of function and mobility following stroke. *Cochrane Database Syst. Rev.* **2014**, *2014*, CD001920.
18. Malwanage, K.T.; Senadheera, V.V.; Dassanayake, T.L. Effect of balance training on footwork performance in badminton: An interventional study. *PLoS ONE* **2022**, *17*, e0277775. [[CrossRef](#)]
19. Lafitte, M.N.; Kadone, H.; Kubota, S.; Shimizu, Y.; Tan, C.K.; Koda, M.; Hada, Y.; Sankai, Y.; Suzuki, K.; Yamazaki, M. Alteration of muscle activity during voluntary rehabilitation training with single-joint Hybrid Assistive Limb (HAL) in patients with shoulder elevation dysfunction from cervical origin. *Front. Neurosci.* **2022**, *16*, 817659. [[CrossRef](#)]
20. Wei, S.; Qiu, X.; An, J.; Chen, Z.; Zhang, X. Highly sensitive, flexible, green synthesized graphene/biomass aerogels for pressure sensing application. *Compos. Sci. Technol.* **2021**, *207*, 108730. [[CrossRef](#)]
21. de Leeuw, A.-W.; Heijboer, M.; Verdonck, T.; Knobbe, A.; Latré, S. Exploiting sensor data in professional road cycling: Personalized data-driven approach for frequent fitness monitoring. *Data Min. Knowl. Discov.* **2023**, *37*, 1125–1153. [[CrossRef](#)]
22. Yang, J.; Lv, W. Optimization of Sports Training Systems Based on Wireless Sensor Networks Algorithms. *IEEE Sens. J.* **2021**, *21*, 25075–25082. [[CrossRef](#)]
23. Li, R.T.; Kling, S.R.; Salata, M.J.; Cupp, S.A.; Sheehan, J.; Voos, J.E. Wearable Performance Devices in Sports Medicine. *Sports Health* **2016**, *8*, 74–78. [[CrossRef](#)]
24. Sun, F.; Zhu, Y.; Jia, C.; Zhao, T.; Chu, L.; Mao, Y. Advances in self-powered sports monitoring sensors based on triboelectric nanogenerators. *J. Energy Chem.* **2023**, *79*, 477–488. [[CrossRef](#)]
25. Lu, Z.; Wen, Y.; Yang, X.; Li, D.; Liu, B.; Zhang, Y.; Zhu, J.; Zhu, Y.; Zhang, S.; Mao, Y. A Wireless Intelligent Motion Correction System for Skating Monitoring Based on a Triboelectric Nanogenerator. *Electronics* **2023**, *12*, 320. [[CrossRef](#)]
26. Lu, Z.; Xie, Z.; Zhu, Y.; Jia, C.; Zhang, Y.; Yang, J.; Zhou, J.; Sun, F.; Mao, Y. A Stable and Durable Triboelectric Nanogenerator for Speed Skating Land Training Monitoring. *Electronics* **2022**, *11*, 3717. [[CrossRef](#)]
27. Mao, Y.; Sun, F.; Zhu, Y.; Jia, C.; Zhao, T.; Huang, C.; Li, C.; Ba, N.; Che, T.; Chen, S. Nanogenerator-Based Wireless Intelligent Motion Correction System for Storing Mechanical Energy of Human Motion. *Sustainability* **2022**, *14*, 6944. [[CrossRef](#)]
28. Lord, S.; Galna, B.; Verghese, J.; Coleman, S.; Burn, D.; Rochester, L. Independent Domains of Gait in Older Adults and Associated Motor and Nonmotor Attributes: Validation of a Factor Analysis Approach. *J. Gerontol. Ser. A* **2013**, *68*, 820–827. [[CrossRef](#)]
29. Chen, S.; Lach, J.; Lo, B.; Yang, G.-Z. Toward Pervasive Gait Analysis With Wearable Sensors: A Systematic Review. *IEEE J. Biomed. Health Inform.* **2016**, *20*, 1521–1537. [[CrossRef](#)]
30. McCarney, L.; Andrews, A.; Henry, P.; Fazalbhoy, A.; Raj, I.S.; Lythgo, N.; Kendall, J.C. Determining Trendelenburg test validity and reliability using 3-dimensional motion analysis and muscle dynamometry. *Chiropr. Man. Ther.* **2020**, *28*, 53. [[CrossRef](#)]
31. Luo, J.; Gao, W.; Wang, Z.L. The Triboelectric Nanogenerator as an Innovative Technology toward Intelligent Sports. *Adv. Mater.* **2021**, *33*, e2004178. [[CrossRef](#)] [[PubMed](#)]
32. Luo, X.; Zhu, L.; Wang, Y.; Li, J.; Nie, J.; Wang, Z.L. A Flexible Multifunctional Triboelectric Nanogenerator Based on MXene/PVA Hydrogel. *Adv. Funct. Mater.* **2021**, *31*, 2104928. [[CrossRef](#)]
33. Hu, S.; Han, J.; Shi, Z.; Chen, K.; Xu, N.; Wang, Y.; Zheng, R.; Tao, Y.; Sun, Q.; Wang, Z.L.; et al. Biodegradable, Super-Strong, and Conductive Cellulose Macrofibers for Fabric-Based Triboelectric Nanogenerator. *Nano-Micro Lett.* **2022**, *14*, 115. [[CrossRef](#)] [[PubMed](#)]
34. Zhang, Q.; Xin, C.; Shen, F.; Gong, Y.; Zi, Y.; Guo, H.; Li, Z.; Peng, Y.; Zhang, Q.; Wang, Z.L. Human body IoT systems based on the triboelectrification effect: Energy harvesting, sensing, interfacing and communication. *Energy Environ. Sci.* **2022**, *15*, 3688–3721. [[CrossRef](#)]

35. Lu, C.; Chen, J.; Jiang, T.; Gu, G.; Tang, W.; Wang, Z.L. A Stretchable, Flexible Triboelectric Nanogenerator for Self-Powered Real-Time Motion Monitoring. *Adv. Mater. Technol.* **2018**, *3*, 1800021. [[CrossRef](#)]
36. Fan, F.R.; Tang, W.; Wang, Z.L. Flexible Nanogenerators for Energy Harvesting and Self-Powered Electronics. *Adv. Mater.* **2016**, *28*, 4283–4305. [[CrossRef](#)]
37. Pu, X.; Li, L.; Song, H.; Du, C.; Zhao, Z.; Jiang, C.; Cao, G.; Hu, W.; Wang, Z.L. A Self-Charging Power Unit by Integration of a Textile Triboelectric Nanogenerator and a Flexible Lithium-Ion Battery for Wearable Electronics. *Adv. Mater.* **2015**, *27*, 2472–2478. [[CrossRef](#)]
38. Wang, J.; Li, S.; Yi, F.; Zi, Y.; Lin, J.; Wang, X.; Xu, Y.; Wang, Z.L. Sustainably powering wearable electronics solely by biomechanical energy. *Nat. Commun.* **2016**, *7*, 12744. [[CrossRef](#)]
39. Zi, Y.; Guo, H.; Wen, Z.; Yeh, M.-H.; Hu, C.; Wang, Z.L. Harvesting Low-Frequency (<5 Hz) Irregular Mechanical Energy: A Possible Killer Application of Triboelectric Nanogenerator. *ACS Nano* **2016**, *10*, 4797–4805.
40. Bai, P.; Zhu, G.; Lin, Z.H.; Jing, Q.S.; Chen, J.; Zhang, G.; Ma, J.; Wang, Z.L. Integrated Multi layered Triboelectric Nanogenerator for Harvesting Biomechanical Energy from Human Motions. *ACS Nano* **2013**, *7*, 3713–3719. [[CrossRef](#)]
41. Su, Y.; Chen, G.; Chen, C.; Gong, Q.; Xie, G.; Yao, M.; Tai, H.; Jiang, Y.; Chen, J. Self-Powered Respiration Monitoring Enabled By a Triboelectric Nanogenerator. *Adv. Mater.* **2021**, *33*, e2101262. [[CrossRef](#)]
42. Guan, X.; Xu, B.; Wu, M.; Jing, T.; Yang, Y.; Gao, Y. Breathable, washable and wearable woven-structured triboelectric nanogenerators utilizing electrospun nanofibers for biomechanical energy harvesting and self-powered sensing. *Nano Energy* **2021**, *80*, 105549. [[CrossRef](#)]
43. Zhang, Q.; Jin, T.; Cai, J.G.; Xu, L.; He TY, Y.; Wang, T.H.; Tian, Y.Z.; Li, L.; Peng, Y.; Lee, C.K. Wearable Triboelectric Sensors Enabled Gait Analysis and Waist Motion Capture for IoT-Based Smart Healthcare Applications. *Adv. Sci.* **2022**, *9*, 2103694. [[CrossRef](#)]
44. Peng, X.; Dong, K.; Ning, C.A.; Cheng, R.W.; Yi, J.; Zhang, Y.H.; Sheng, F.F.; Wu, Z.Y.; Wang, Z.L. All-Nanofiber Self-Powered Skin-Interfaced Real-Time Respiratory Monitoring System for Obstructive Sleep Apnea-Hypopnea Syndrome Diagnosing. *Adv. Funct. Mater.* **2021**, *31*, 2103559. [[CrossRef](#)]
45. Jiang, Y.; An, J.; Liang, F.; Zuo, G.; Yi, J.; Ning, C.; Zhang, H.; Dong, K.; Wang, Z.L. Knitted self-powered sensing textiles for machine learning-assisted sitting posture monitoring and correction. *Nano Res.* **2022**, *15*, 8389–8397. [[CrossRef](#)]
46. Luo, H.; Wang, H.; Yang, L.; Wu, H.; Kang, S.; Yong, S.; Liao, R.; Wang, J.; Wang, Z.L. In Situ Nanofluid Dispersion Monitoring by Liquid–Solid Triboelectric Nanogenerator Based on Tuning the Structure of the Electric Double Layer. *Adv. Funct. Mater.* **2022**, *32*, 2200862. [[CrossRef](#)]
47. Chen, M.; Zhou, Y.; Lang, J.; Li, L.; Zhang, Y. Triboelectric nanogenerator and artificial intelligence to promote precision medicine for cancer. *Nano Energy* **2022**, *92*, 106783. [[CrossRef](#)]
48. Wang, S.; Tian, M.; Hu, S.; Zhai, W.; Zheng, G.; Liu, C.; Shen, C.; Dai, K. Hierarchical nanofibrous mat via water-assisted electrospinning for self-powered ultrasensitive vibration sensors. *Nano Energy* **2022**, *97*, 107149. [[CrossRef](#)]
49. Lu, Z.; Jia, C.; Yang, X.; Zhu, Y.; Sun, F.; Zhao, T.; Zhang, S.; Mao, Y. A Flexible TENG Based on Micro-Structure Film for Speed Skating Techniques Monitoring and Biomechanical Energy Harvesting. *Nanomaterials* **2022**, *12*, 1576. [[CrossRef](#)]
50. Zhao, T.; Fu, Y.; Sun, C.; Zhao, X.; Jiao, C.; Du, A.; Wang, Q.; Mao, Y.; Liu, B. Wearable biosensors for real-time sweat analysis and body motion capture based on stretchable fiber-based triboelectric nanogenerators. *Biosens. Bioelectron.* **2022**, *205*, 114115. [[CrossRef](#)]
51. Mao, Y.; Zhu, Y.; Jia, C.; Zhao, T.; Zhu, J. A Self-Powered Flexible Biosensor for Human Exercise Intensity Monitoring. *J. Nanoelectron.* **2021**, *16*, 699–706. [[CrossRef](#)]
52. Lu, Z.; Zhu, Y.; Jia, C.; Zhao, T.; Bian, M.; Jia, C.; Zhang, Y.; Mao, Y. A Self-Powered Portable Flexible Sensor of Monitoring Speed Skating Techniques. *Biosensors* **2021**, *11*, 108. [[CrossRef](#)] [[PubMed](#)]
53. Zheng, N.; Xue, J.; Jie, Y.; Cao, X.; Wang, Z.L. Wearable and humidity-resistant biomaterials-based triboelectric nanogenerator for high entropy energy harvesting and self-powered sensing. *Nano Res.* **2022**, *15*, 6213–6219. [[CrossRef](#)]
54. Lin, Z.; Wu, Z.; Zhang, B.; Wang, Y.-C.; Guo, H.; Liu, G.; Chen, C.; Chen, Y.; Yang, J.; Wang, Z.L. A Triboelectric Nanogenerator-Based Smart Insole for Multifunctional Gait Monitoring. *Adv. Mater. Technol.* **2019**, *4*, 1800360. [[CrossRef](#)]
55. Mao, Y.; Yue, W.; Zhao, T.; Shen, M.L.; Liu, B.; Chen, S. A Self-Powered Biosensor for Monitoring Maximal Lactate Steady State in Sport Training. *Biosensors* **2020**, *10*, 75. [[CrossRef](#)]
56. Jia, C.; Zhu, Y.; Sun, F.; Wen, Y.; Wang, Q.; Li, Y.; Mao, Y.; Zhao, C. Gas-Supported Triboelectric Nanogenerator Based on In Situ Gap-Generation Method for Biomechanical Energy Harvesting and Wearable Motion Monitoring. *Sustainability* **2022**, *14*, 14422. [[CrossRef](#)]
57. Zhu, Y.; Sun, F.; Jia, C.; Huang, C.; Wang, K.; Li, Y.; Chou, L.; Mao, Y. A 3D Printing Triboelectric Sensor for Gait Analysis and Virtual Control Based on Human–Computer Interaction and the Internet of Things. *Sustainability* **2022**, *14*, 10875. [[CrossRef](#)]

**Disclaimer/Publisher’s Note:** The statements, opinions and data contained in all publications are solely those of the individual author(s) and contributor(s) and not of MDPI and/or the editor(s). MDPI and/or the editor(s) disclaim responsibility for any injury to people or property resulting from any ideas, methods, instructions or products referred to in the content.